HHS Public Access

Author manuscript

Nat Cell Biol. Author manuscript; available in PMC 2013 May 01.

Published in final edited form as:

Nat Cell Biol. 2012 November ; 14(11): 1139–1147. doi:10.1038/ncb2603.

Nanog-dependent feedback loops regulate murine embryonic stem cell heterogeneity

Ben D. MacArthur[1,2,3,*], **Ana Sevilla**[4,5,*], **Michel Lenz**[6], **Franz-Josef Müller**[7], **Berhard M. Schuldt**[6], **Andreas A. Schuppert**[6], **Sonya J. Ridden**[2,8], **Patrick S. Stumpf**[1], **Miguel Fidalgo**[4,5], **Avi Ma'ayan**[9], **Jianlong Wang**[4,5], and **Ihor R. Lemischka**[4,5,9]

[1]Centre for Human Development, Stem Cells and Regeneration, Institute of Developmental Sciences, University of Southampton, Southampton, SO17 1BJ, UK

[2]School of Mathematics, University of Southampton, Southampton, SO17 1BJ, UK

[3]Institute for Life Sciences, University of Southampton, SO17 1BJ, UK

[4]Department of Developmental and Regenerative Biology, Mount Sinai School of Medicine, New York, New York, 10029, USA

[5]Black Family Stem Cell Institute, Mount Sinai School of Medicine, New York, New York, 10029, USA

[6]Aachen Institute for Advanced Study in Computational Engineering Science, Rheinisch-Westfälische Technische Hochschule Aachen, Aachen, Germany

[7]Zentrum für Integrative Psychiatrie, Kiel, Germany

[8]Institute for Complex Systems Simulation, University of Southampton, UK

[9]Department of Pharmacology and Systems Therapeutics, Mount Sinai School of Medicine, New York, New York, 10029, USA

Abstract

A number of key regulators of mouse embryonic stem (ES) cell identity, including the transcription factor Nanog, show strong expression fluctuations at the single cell level. The molecular basis for these fluctuations is unknown. Here we used a genetic complementation strategy to investigate expression changes during transient periods of Nanog downregulation.

Correspondence and requests for materials should be addressed to Ben MacArthur (B.D.MacArthur@soton.ac.uk), Ana Sevilla (ana.sevilla@mssm.edu) and Ihor Lemischka (ihor.lemischka@mssm.edu).

*These authors contributed equally to this work

Accession Codes

Primary accessions: All microarray data are deposited at the Gene Expression Omnibus (GEO) database repository under accession number GSE40335.

Referenced accessions: GSE34243 (GEO). Further accession codes are given in Supplementary Table S3.

Author Contributions

BDM, AS and IRL designed the project and prepared the manuscript. AS, MF and JW performed the experiments. BDM, ML, FJM, BMS, AAS, SJR, PSS and AM performed the bioinformatic analyses and mathematical modelling. All authors reviewed and approved the manuscript.

The authors declare no competing financial interests.

Employing an integrated approach, that includes high-throughput single cell transcriptional profiling and mathematical modelling, we found that early molecular changes subsequent to Nanog loss are stochastic and reversible. However, analysis also revealed that Nanog loss severely compromises the self-sustaining feedback structure of the ES cell regulatory network. Consequently, these nascent changes soon become consolidated to committed fate decisions in the prolonged absence of Nanog. Consistent with this, we found that exogenous regulation of Nanog-dependent feedback control mechanisms produced more a homogeneous ES cell population. Taken together our results indicate that Nanog-dependent feedback loops have a role in controlling both ES cell fate decisions and population variability.

Several important regulators of ES cell identity, including the homeodomain transcription factor Nanog[1–3], show significant temporal expression fluctuations at the single cell level[4–15]. Such fluctuations give rise to robust functional heterogeneity within ES cell populations, profoundly affecting their long-term regenerative potency[9,16,17]. In the case of Nanog, apparently stochastic transitions between Nanog-high and Nanog-low states occur within individual Oct4 positive ES cells[13]. These fluctuations transiently prime individual ES cells for differentiation without marking definitive commitment[4]. Thus, Nanog appears to act as a molecular “gatekeeper”: suppressing adverse spontaneous differentiation events in fluctuating environments while ensuring robust differentiation in the presence of appropriate and persistent stimuli. However, the molecular basis for this mechanism remains unclear.

In order to investigate this issue we developed a time-course strategy designed to controllably reproduce the Nanog expression level fluctuations observed in wild-type ES cells[7,17]. To accurately regulate Nanog levels we used the doxycycline (dox) dependent inducible system previously described[18,19] (Fig. 1a). In this system a short hairpin RNA (shRNA) depletes endogenous *Nanog* mRNA, while normal levels of Nanog are restored from a dox-inducible shRNA “immune” mRNA[18,19]. In the presence of dox this engineered “rescue” mouse ES cell line (NanogR) expresses Nanog homogeneously (Fig. 1b) and is fully pluripotent both *in vitro* and *in vivo*[18,19]. Upon removal of dox, *Nanog* mRNA and protein levels sharply decline and pluripotency and self-renewal capacities are progressively lost[18,19]. Cell samples were harvested at day 0 (dox present, Nanog expressing) and at days 1, 3, and 5 days after dox withdrawal (Fig. 1c). Additionally, at each time-point a set of samples was further treated with a twelve-hour pulse of dox before being harvested and compared with untreated control samples harvested at the same time. Thus, cells were exposed to transient periods (24, 72 and 120 hours) of Nanog removal. In essence, this strategy mimics the reported temporal fluctuations of endogenous Nanog expression levels[4,13]. Gene expression microarrays were performed in triplicate at each time point and culture condition to determine the effects of Nanog fluctuations on global mRNA levels (Fig. 2).

Results

Identifying a critical “point-of-no-return” in the ES cell fate switch

Expression of pluripotency-associated transcripts was progressively downregulated upon Nanog removal (Figs. 1d-e and 2b). In order to provide context to these changes we considered them in light of two previously published regulatory networks for ES cell pluripotency: a transcriptional regulatory network (TRN) (as detailed in Ref. 20) and an extended ES cell regulatory network (as detailed in Ref. 21 and updated in Supplementary Table S1). While Nanog was robustly downregulated within 24 hours of dox removal (without dox Nanog is almost undetectable after 1 day, see Fig. 1d–e and Fig. 2b), most elements of both the TRN and the extended network did not show significant changes in expression until at least 3 days after Nanog depletion (Fig. 1d–e, Fig. 2b, and Supplementary Fig. S2). This indicates that loss of pluripotency occurs on a timescale significantly longer than that of Nanog loss. Indeed, consistent with previous observations[4,22], full decomposition of the ES cell TRN was only observed after 5 days (Fig. 1 d–e), indicating that this network remains essentially active in the temporary absence of Nanog[4]. Once significant expression changes had occurred (day 3 onwards), reintroduction of Nanog did not have a significant rescue effect on most pluripotency markers (Fig. 1d–e and Fig. 2b), suggesting that a critical point had been passed and that permanent changes in the TRN had occurred. To investigate this further we constructed a simple mathematical model of Nanog regulation of pluripotency. Analysis of this model suggests that the observed dynamics are due to a bistable switch in which Nanog plays a central role by positively reinforcing the pluripotent ground[3,23] state (see Supplementary note 1 for full details).

Lineage associated gene expression changes are reversible

Markers of the earliest mammalian lineages (trophoblast, primitive endoderm and primitive ectoderm/neural ectoderm) (as detailed in Ref. 24 and given in Supplementary Table S1) as well as cell cycle checkpoint-associated genes (Supplementary Table S1) showed significant upregulation within 36 hours of Nanog removal, indicating that Nanog is a potent negative regulator of early lineage decisions[4,19] and cell cycle checkpoint controls[25]. Furthermore, both lineage and pluripotency-associated markers were significantly enriched within the set of genes that exhibited significant expression changes upon Nanog removal (Supplementary Table S2). However, in contrast to expression changes of pluripotency-associated genes, changes in early lineage-associated genes were rapidly reversible upon reintroduction of Nanog (Fig. 2b), indicating a gradual and revocable accumulation of lineage characteristics. A similar pattern of reversible expression changes was also observed in germ cell associated genes, in accordance with the central role that Nanog plays in primordial germ cell identity[4] (Supplementary Fig. S2).

A bioinformatic classifier for pluripotency of mouse cells

In order to gain a better understanding of these early fate changes we developed a bioinformatic assay for pluripotency of mouse cells[26]. We first downloaded and manually curated a training set of 1032 mouse microarray datasets from the Gene Expression Omnibus (GEO) database (http://www.ncbi.nlm.nih.gov/geo/), including expression profiles of pluripotent cells (142 samples) and a variety of somatic cell samples (790 samples)

(Supplementary Table S3). We then developed two machine-learning classifiers (full details and code are given in Supplementary note 2 and Supplementary Software) which, when taken together, were able to accurately distinguish pluripotent from non-pluripotent samples in our training dataset (Fig. 2c, left panel). The first classifier, termed the "Pluripotency Score", identifies patterns of gene expression specifically associated with pluripotency. The second, termed the "Lineage Score", determines if novel expression patterns not observed in the pluripotent training samples are present. Thus, pluripotent cells have a high Pluripotency Score and a low Lineage Score; while somatic cells have the converse Scores (Fig. 2c, left panel). In contrast to focused gene sets (Fig. 2b), the Pluripotency and Lineage Scores are complex genome-wide biomarkers that measure global transcriptional patterns associated with pluripotent and somatic cells[27] and it is the combined use of these two scores which allows separation of pluripotent from somatic samples (see Supplementary note 2 for further discussion). Application of these classifiers confirmed a gradual movement away from the (day 0) pluripotent state (Fig. 2c, right panel and Fig. 2d). However, while the Lineage Score progressively increased following Nanog removal, indicating a gradual increase in acquired lineage characteristics, the Pluripotency Score showed a transient increase, remaining high 3 days after removal of Nanog, before decreasing (Fig. 2c, right panel). Principal component analysis (PCA) of the time-course data also revealed a similar pattern (Fig. 2e). Comparable dynamics have previously been noted during neural differentiation of human ES cells and induced pluripotent stem (iPS) cells[26]. To gain a better understanding of this transient increase in the Pluripotency Score, we reanalyzed a previously published dataset from an *in vitro* differentiation time-course of murine ES cell cultures to pluripotent epiblast stem cells[28] and observed a similar increase in the Pluripotency Score (see Supplementary note 2 for further details). Thus, a transient Pluripotency Score increase appears to be characteristic of movement from a relatively naïve ES cell state[3,23] to a poised cellular intermediate in which early differentiation programs and pluripotency circuitry run in parallel.

Gene expression changes are regulated in a combinatorial manner

In order to better determine the molecular mechanisms underpinning these observations we compared target gene expression changes with previously published promoter occupancy data[20] for each of the elements of the ES cell TRN (Fig. 3 and Fig. 4). We found that many genes with significant expression changes upon Nanog removal are direct targets of Nanog (Fig. 3a–c) and other members of the extended ES cell TRN (Fig. 3d, Fig. 4 and Supplementary Table S4). In accordance with previous observations[20] we found highly combinatorial regulation of target gene expression, with less than 1% of significantly changing genes being regulated by Nanog alone (Supplementary Table S4). In total, we identified 126 unique coregulatory patterns (enumerated in full in Supplementary Table S4), indicating that the genome-wide changes that occur subsequent to Nanog removal are mediated via the combinatorial action of multiple factors. In accordance with this, we found that overall rescue efficiency (see online Methods for details) also progressively diminished subsequent to Nanog removal as the core TRN shuts down (Fig. 4).

Taken together, these results indicate that mouse ES cells adopt a reversible "primed" state during short-lived downregulation of Nanog, characterized by promiscuous coexpression of

pluripotency and early lineage markers as well as nascent engagement of cell cycle checkpoints. However, in the continued absence of Nanog these changes become consolidated into committed fate decisions with an irrevocable downregulation of pluripotency genes and a concomitant upregulation of differentiation genes.

Early fate changes are stochastic and reversible at the single cell level

Since a number of key ES cell genes, including members of the core ES cell TRN such as *Nanog*, *Rex1*, and *Klf4*, are heterogeneously expressed at the single cell level[4–15] we reasoned that population-based microarray data might mask important cell-cell variability. In order to gain better insight into the molecular changes accompanying transient Nanog removal we conducted high-throughput single cell transcriptional profiling. Time-lapse microscopy of individual ES cells has previously shown that stochastic fluctuations into a Nanog-low state last approximately 24 hours[13]. This timescale is consistent both with our observation that Nanog protein levels fall dramatically within 24 hours of Nanog downregulation[18] and the relative instability of Nanog protein ($t_{1/2}$ ~ 2 hrs.[29]). Therefore, we sought to further investigate the effects of Nanog fluctuations over this natural 24-hour timescale. We used the BioMark 96.96 Dynamic Array platform (Fluidigm) to profile a panel of 77 genes (Supplementary Table S5), including housekeeping, pluripotency, early lineage and cell cycle associated markers, in cells harvested at 0 hours (dox present, Nanog expressing, denoted 0hrs), 24 and 36 hours after dox withdrawal (denoted 24hrs and 36hrs respectively) and treated with a 12 hour pulse of dox after 24 hours without dox (denoted 36hrsR) (Fig. 5). In total, 384 individual cells were profiled covering these different time points. Overall, expression patterns derived from single cells showed a good correspondence with microarray population-based profiles and exhibited a nontrivial covariance structure (for a full discussion see Supplementary note 2). Flow-cytometric single cell analysis confirmed both efficient, synchronous downregulation of Nanog upon dox removal, and efficient, synchronous rescue of its expression upon reintroduction of dox (Fig. 5b). Consistent with previous publications[4–7,13,30] we found that mouse ES cells are highly heterogeneous with respect to their overall expression profiles (Fig. 5a). Single cell analysis confirmed transient upregulation of transcripts associated with early differentiation and cell cycle checkpoints upon Nanog removal (Fig. 5a). Moreover, unsupervised clustering failed to identify discrete subpopulations (Fig. 5a), indicating that the early stages of differentiation subsequent to Nanog depletion occur as a gradual stochastic population drift rather than a collective and synchronous transition. A similar phenomenon was recently observed using high-throughput transcriptional profiling of single cells during haematopoiesis[31], suggesting that stochasticity in commitment may be an inherent feature of mammalian development. Although distinct clusters were not identified using unsupervised approaches, a distinction was apparent using a Support Vector Machine (SVM) classifier[32] using the 0hr and 36hr datasets to train the benchmark “pluripotent” and “lineage primed” classes, respectively (Fig. 5c). A training misclassification rate (MCR) of 4% was achieved, indicating the presence of different patterns of expression in the two training samples. However, using this SVM only 45% of the 24hr cells were classified as pluripotent (Fig. 5c left panel), indicating that early fate changes are stochastic at the single cell level, while 72% of the 36hrsR cells were classified as pluripotent (Fig. 5c right panel), indicating robust reversibility at this early stage.

Feedback loops regulate ES cell fate commitment

Feedback loops (which can be positive, negative or mixed) commonly regulate phenotypic variability in diverse organisms and contexts by generating complex dynamics[33], such as multi-stability[34–39], excitability[13] and oscillations[40–42], and by modulating molecular noise[43,44]. Accordingly, we reasoned that Nanog fluctuations might regulate early cell fate decisions and population variability by controlling feedback mechanisms in the ES cell TRN. To investigate this possibility we analysed the feedback structure of the extended ES cell TRN[20] (Fig. 6). We found that this network is rich in feedback, containing a total of 28 distinct feedback loops (full details in Supplementary Table S6). Furthermore, these feedback loops are not evenly distributed (Fig. 6c). Rather, the global feedback structure of this network is highly nested and is critically dependent upon Nanog, Oct4 and Sox2 which participate in 68% (19/28), 68% (19/28) and 64% (18/28) of all feedback loops, respectively (see Supplementary Table S6). Calculation of a simple "returnability" index[45,46] (see online Methods for details), which takes into account both the total number and the lengths of all closed paths present in the extended TRN, identified Nanog as the most central element in the global feedback structure (Fig. 6d). Removal of Nanog therefore severely compromises overall feedback structure, leaving only 32% (9/28) of the feedback loops intact. Consequently, fluctuations in Nanog expression levels transiently activate different sub-networks in the ES cell TRN[30], driving transitions between a (Nanog expressing) feedback-rich, robust and self-perpetuating pluripotent state and a (Nanog-diminished), feedback-sparse and differentiation-sensitive state.

We note that while the feedback structure of the extended TRN is severely compromised upon removal of Nanog, it is not entirely destroyed: a small number of key feedback loops still remain, most notably those involving Oct4, Sox2, Dax1 and Rex1 (but not Nanog, see Supplementary Table S6). This may explain why, although they are prone to differentiate, ES cells can be maintained in a self-renewing state in the absence of Nanog[4]. In this situation self-renewing ES cells may adapt to rely on a compromised feedback structure. This also underscores the remarkably robust nature of the pluripotency TRN, and it will be interesting to see if ES cells can similarly adapt to loss of other network components; specifically, those with similar fluctuation properties.

Feedback loops regulate ES cell heterogeneity

In order to further assess the role of feedback in population heterogeneity we compared single cell expression patterns in NanogR cells and in CCE wild-type ES cells. The wild-type ES cell TRN is self-perpetuating when shielded from differentiation-inducing stimuli[23]. However, in the NanogR cell line endogenous regulation of the *Nanog* gene does not contribute to Nanog protein levels. Consequently, all feedback loops that involve Nanog in the wild-type TRN are absent in the NanogR cells. In these cells the ES cell TRN is therefore effectively held in a feedback-depleted state (Fig. 6b) and maintenance of pluripotency is dependent on continued exogenous expression of Nanog rather than activation of self-perpetuating feedback loops. Importantly, NanogR cells are fully pluripotent and capable of producing germ-line chimeras[19]. This highlights the largely dispensable nature of the complex endogeneous feedback architecture in regulating pluripotency.

To investigate the effect of these changes to the TRN on cell-cell variability we compared single cell expression patterns of 31 key pluripotency markers (Supplementary Table S7) in NanogR cells (grown in dox) with those in wild-type CCE ES cells. Overall, NanogR and CCE cells exhibited similar levels of marker expression (Fig. 7a,c), although they could be separated with a SVM classifier (9% MCR) (Fig. 7b), indicating some differences in expression patterns. However, we found that NanogR cells are less variable than CCE cells in overall marker expression patterns ($p = 0.05$ by a multivariate analogue of Levene's test for equality of variances, see online Methods for details) (Fig. 7d) suggesting that the feedback architecture of the ES cell TRN plays a role in controlling cell-cell variability.

Discussion

Previously we have shown that removing Nanog results in a complex mixture of lineages[18,19]. The precise single gene perturbation we have used in this study does not therefore reflect the full complexity of ES cell differentiation *in vivo*. Nevertheless, by initiating differentiation in a precise and tightly controlled manner, this model system provides a powerful means to study the early stages of differentiation. Taken together, our results indicate that Nanog-dependent feedback loops in the ES cell TRN play a role in controlling early fate changes at the single cell level and heterogeneity at the population level. What role might feedback-controlled population heterogeneity play? We suggest that distinct individual states of a fluctuating TRN may reflect a variety of coexisting lineage "primed" differentiation tendencies that can respond to the presence of powerful stimuli. This remains to be tested; however, a better understanding of the role of feedback in controlling ES cells will facilitate the maintenance of more defined pluripotent populations and the development of more robust differentiation protocols.

Supplementary Material

Refer to Web version on PubMed Central for supplementary material.

Acknowledgments

We thank Konrad Hochedlinger for the Nanog-GFP mouse ES cells[47]. We gratefully acknowledge funding support by NIH (GM078465) and NYSTEM (C024410) to IRL. This work was also supported by an EPSRC Doctoral Training Centre grant (EP/G03690X/1) and an EPSRC 2011/12 Institutional Sponsorship Award (EP/J501530/1).

References

1. Chambers I, et al. Functional expression cloning of Nanog, a pluripotency sustaining factor in embryonic stem cells. Cell. 2003; 113:643–655. [PubMed: 12787505]
2. Mitsui K, et al. The homeoprotein Nanog is required for maintenance of pluripotency in mouse epiblast and ES cells. Cell. 2003; 113:631–642. [PubMed: 12787504]
3. Silva J, et al. Nanog Is the Gateway to the Pluripotent Ground State. Cell. 2009; 138:722–737. [PubMed: 19703398]
4. Chambers I, et al. Nanog safeguards pluripotency and mediates germline development. Nature. 2007; 450:1230–U1238. [PubMed: 18097409]
5. Canham MA, Sharov AA, Ko MSH, Brickman JM. Functional Heterogeneity of Embryonic Stem Cells Revealed through Translational Amplification of an Early Endodermal Transcript. Plos Biol. 2010; 8

6. Toyooka Y, Shimosato D, Murakami K, Takahashi K, Niwa H. Identification and characterization of subpopulations in undifferentiated ES cell culture. Development. 2008; 135:909–918. [PubMed: 18263842]
7. Hayashi K, Lopes SMCD, Tang F, Surani MA. Dynamic Equilibrium and Heterogeneity of Mouse Pluripotent Stem Cells with Distinct Functional and Epigenetic States. Cell Stem Cell. 2008; 3:391–401. [PubMed: 18940731]
8. Trott J, Hayashi K, Surani A, Babu MM, Martinez-Arias A. Dissecting ensemble networks in ES cell populations reveals micro-heterogeneity underlying pluripotency. Mol Biosyst. 2012; 8:744–752. [PubMed: 22222461]
9. Macfarlan TS, et al. Embryonic stem cell potency fluctuates with endogenous retrovirus activity. Nature. 2012; 487:57–63. [PubMed: 22722858]
10. Niakan KK, et al. Sox17 promotes differentiation in mouse embryonic stem cells by directly regulating extraembryonic gene expression and indirectly antagonizing self-renewal. Gene Dev. 2010; 24:312–326. [PubMed: 20123909]
11. Singh AM, Hamazaki T, Hankowski KE, Terada N. A heterogeneous expression pattern for nanog in embryonic stem cells. Stem Cells. 2007; 25:2534–2542. [PubMed: 17615266]
12. Zalzman M, et al. Zscan4 regulates telomere elongation and genomic stability in ES cells. Nature. 2010; 464:858–U866. [PubMed: 20336070]
13. Kalmar T, et al. Regulated Fluctuations in Nanog Expression Mediate Cell Fate Decisions in Embryonic Stem Cells. Plos Biol. 2009; 7
14. Kobayashi T, et al. The cyclic gene Hes1 contributes to diverse differentiation responses of embryonic stem cells. Gene Dev. 2009; 23:1870–1875. [PubMed: 19684110]
15. Niwa H, Ogawa K, Shimosato D, Adachi K. A parallel circuit of LIF signalling pathways maintains pluripotency of mouse ES cells. Nature. 2009; 460:118–122. [PubMed: 19571885]
16. Arias AM, Brickman JM. Gene expression heterogeneities in embryonic stem cell populations: origin and function. Curr Opin Cell Biol. 2011; 23:650–656. [PubMed: 21982544]
17. Stewart MH, Bendall SC, Levadoux-Martin M, Bhatia M. Clonal tracking of hESCs reveals differential contribution to functional assays. Nat Methods. 2010; 7:917–U975. [PubMed: 20953174]
18. Lu R, et al. Systems-level dynamic analyses of fate change in murine embryonic stem cells. Nature. 2009; 462:358–U126. [PubMed: 19924215]
19. Ivanova N, et al. Dissecting self-renewal in stem cells with RNA interference. Nature. 2006; 442:533–538. [PubMed: 16767105]
20. Kim J, Chu JL, Shen XH, Wang JL, Orkin SH. An extended transcriptional network for pluripotency of embryonic stem cells. Cell. 2008; 132:1049–1061. [PubMed: 18358816]
21. Muller FJ, et al. Regulatory networks define phenotypic classes of human stem cell lines. Nature. 2008; 455:401–U455. [PubMed: 18724358]
22. Ramirez JM, et al. Brief Report: Benchmarking Human Pluripotent Stem Cell Markers During Differentiation Into the Three Germ Layers Unveils a Striking Heterogeneity: All Markers Are Not Equal. Stem Cells. 2011; 29:1469–1474. [PubMed: 21714037]
23. Ying QL, et al. The ground state of embryonic stem cell self-renewal. Nature. 2008; 453:519–U515. [PubMed: 18497825]
24. Aiba L, et al. Defining Developmental Potency and Cell Lineage Trajectories by Expression Profiling of Differentiating Mouse Embryonic Stem Cells. DNA Res. 2009; 16:73–80. [PubMed: 19112179]
25. Zhang X, et al. A role for NANOG in G1 to S transition in human embryonic stem cells through direct binding of CDK6 and CDC25A. J Cell Biol. 2009; 184:67–82. [PubMed: 19139263]
26. Muller FJ, et al. A bioinformatic assay for pluripotency in human cells. Nat Methods. 2011; 8:315–U354. [PubMed: 21378979]
27. Williams R, Schuldt B, Muller FJ. A guide to stem cell identification: Progress and challenges in system-wide predictive testing with complex biomarkers. Bioessays. 2011; 33:880–890. [PubMed: 21901750]

28. Nora EP, et al. Spatial partitioning of the regulatory landscape of the X-inactivation centre. Nature. 2012; 485:381–385. [PubMed: 22495304]
29. Ramakrishna S, et al. PEST Motif Sequence Regulating Human NANOG for Proteasomal Degradation. Stem Cells Dev. 2011; 20:1512–1520.
30. Xiong W, Ferrell JE. A positive-feedback-based bistable 'memory module' that governs a cell fate decision. Nature. 2003; 426:460–465. [PubMed: 14647386]
31. Pina C, et al. Inferring rules of lineage commitment in haematopoiesis. Nat Cell Biol. 2012; 14:287–294. [PubMed: 22344032]
32. Cristianini, N.; Shawe-Taylor, J. An Introduction to Support Vector Machines and Other Kernel-based Learning Methods. Cambridge University Press; 2000.
33. Tyson JJ, Chen KC, Novak B. Sniffers, buzzers, toggles and blinkers: dynamics of regulatory and signaling pathways in the cell. Curr Opin Cell Biol. 2003; 15:221–231. [PubMed: 12648679]
34. Smits WK, Kuipers OP, Veening JW. Phenotypic variation in bacteria: the role of feedback regulation. Nat Rev Microbiol. 2006; 4:259–271. [PubMed: 16541134]
35. Ferrell JE. Self-perpetuating states in signal transduction: positive feedback, double-negative feedback and bistability. Curr Opin Cell Biol. 2002; 14:140–148. [PubMed: 11891111]
36. Becskei A, Seraphin B, Serrano L. Positive feedback in eukaryotic gene networks: cell differentiation by graded to binary response conversion. Embo J. 2001; 20:2528–2535. [PubMed: 11350942]
37. MacArthur BD, Ma'ayan A, Lemischka IR. Systems biology of stem cell fate and cellular reprogramming. Nat Rev Mol Cell Bio. 2009; 10:672–681. [PubMed: 19738627]
38. MacArthur BD, Please CP, Oreffo ROC. Stochasticity and the Molecular Mechanisms of Induced Pluripotency. Plos One. 2008; 3
39. MacArthur BD, Ma'ayan A, Lemischka IR. Toward Stem Cell Systems Biology: From Molecules to Networks and Landscapes. Cold Sh Q B. 2008; 73:211–215.
40. Tigges M, Marquez-Lago TT, Stelling J, Fussenegger M. A tunable synthetic mammalian oscillator. Nature. 2009; 457:309–312. [PubMed: 19148099]
41. Elowitz MB, Leibler S. A synthetic oscillatory network of transcriptional regulators. Nature. 2000; 403:335–338. [PubMed: 10659856]
42. Glauche I, Herberg M, Roeder I. Nanog Variability and Pluripotency Regulation of Embryonic Stem Cells - Insights from a Mathematical Model Analysis. Plos One. 2010; 5
43. Austin DW, et al. Gene network shaping of inherent noise spectra. Nature. 2006; 439:608–611. [PubMed: 16452980]
44. Paulsson J. Summing up the noise in gene networks. Nature. 2004; 427:415–418. [PubMed: 14749823]
45. Estrada E, Rodriguez-Velazquez JA. Subgraph centrality in complex networks. Phys Rev E. 2005; 71
46. Estrada E, Hatano N. Returnability in complex directed networks (digraphs). Linear Algebra Appl. 2009; 430:1886–1896.
47. Maherali N, et al. Directly reprogrammed fibroblasts show global epigenetic remodeling and widespread tissue contribution. Cell Stem Cell. 2007; 1:55–70. [PubMed: 18371336]
48. Loh YH, et al. The Oct4 and Nanog transcription network regulates pluripotency in mouse embryonic stem cells. Nat Genet. 2006; 38:431–440. [PubMed: 16518401]
49. Cole MF, Johnstone SE, Newman JJ, Kagey MH, Young RA. Tcf3 is an integral component of the core regulatory circuitry of embryonic stem cells. Gene Dev. 2008; 22:746–755. [PubMed: 18347094]
50. Chen X, et al. Integration of external signaling pathways with the core transcriptional network in embryonic stem cells. Cell. 2008; 133:1106–1117. [PubMed: 18555785]
51. Marson A, et al. Connecting microRNA genes to the core transcriptional regulatory circuitry of embryonic stem cells. Cell. 2008; 134:521–533. [PubMed: 18692474]
52. Mathur D, et al. Analysis of the mouse embryonic stem cell regulatory networks obtained by ChIP-chip and ChIP-PET. Genome Biol. 2008; 9

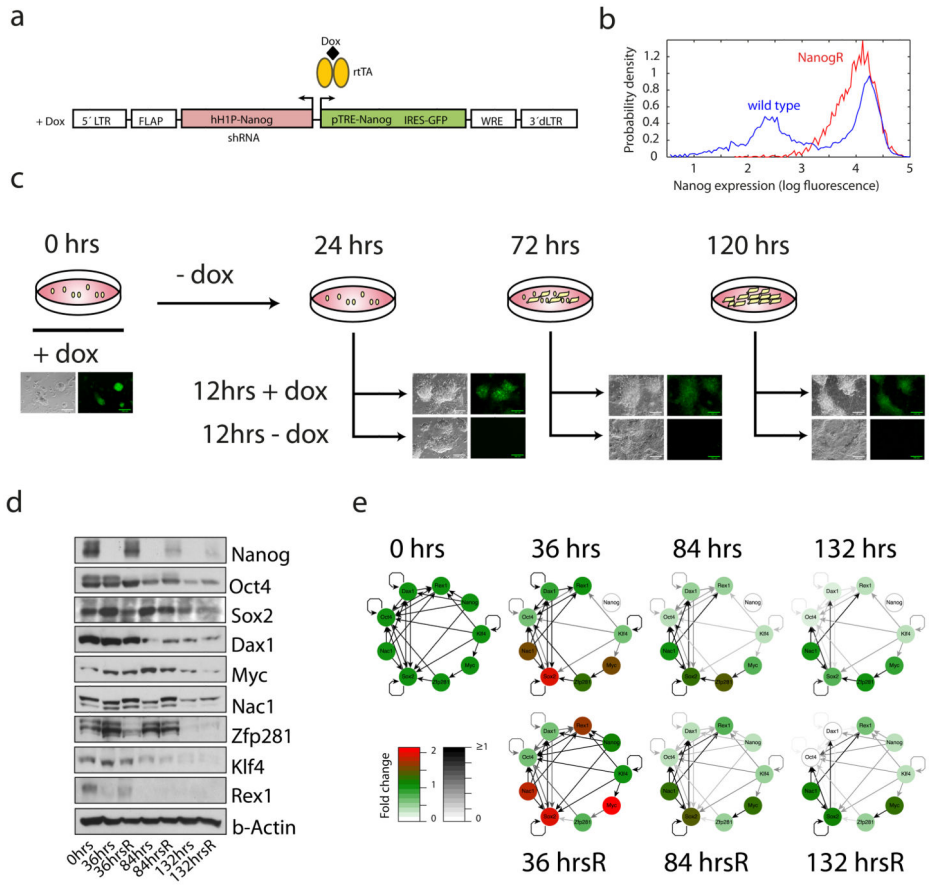

Figure 1. Quantifying the molecular effects of Nanog fluctuations

(a) The lentiviral vector construct to conditionally regulate Nanog expression levels[19]: dLTR, deleted long-terminal repeat; FLAP, sequence element that improves transduction efficiency; rtTA, a TetOn tetracycline (doxycycline)-controlled transcriptional activator; WRE, woodchuck hepatitis virus post-transcriptional regulatory element. **(b)** Flow-cytometric comparison of the distribution of Nanog expression levels in wild-type Nanog GFP[54] and NanogR[19] ES cells. In both cases, GFP levels reflect Nanog levels. **(c)** Experimental design. Scale bar 100 μm. **(d)** Effect of Nanog downregulation and rescue on protein expression levels in the ES cell TRN as measured by western blot. Full scans are given in Supplementary Fig. S1 **(e)** Decomposition of the extended ES cell TRN after Nanog depletion. Colours and grayscale denote relative expression levels measured by qPCR.

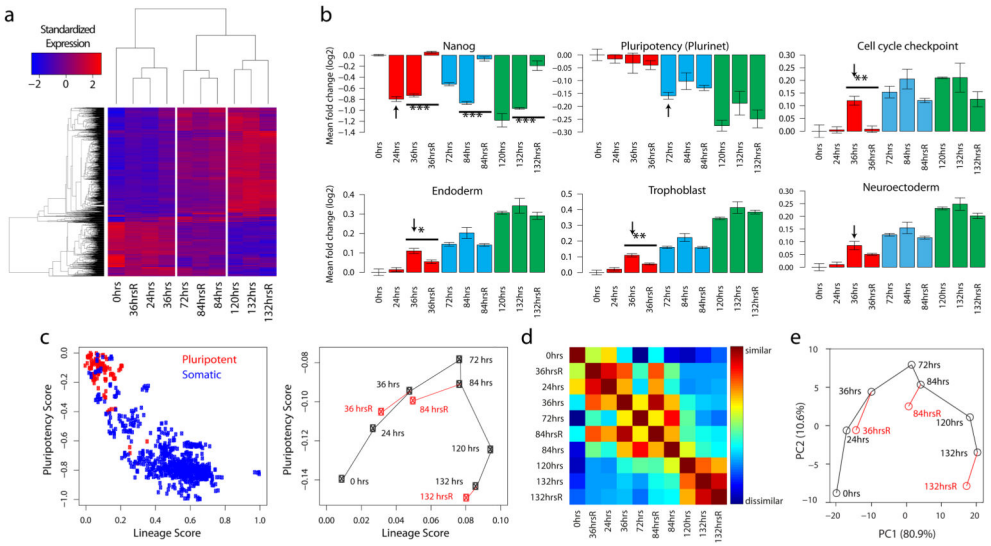

Figure 2. Transcriptome changes during periods of transient Nanog depletion

(a) Heat map of significant gene expression changes. **(b)** Mean fold expression changes for pluripotency (elements of the extended ES cell regulatory network as detailed in Ref. 21 and updated in Supplementary Table S1), cell cycle and lineage associated gene sets. Stars indicate significance by 2 sample t-test with *p*-values: * < 0.05, ** < 0.01, *** < 0.0001; arrows indicate earliest time at which a significant expression change was observed ($p < 0.05$). Error bars show ± one standard error, $n = 3$. **(c)** Machine-learning classification of genome-wide expression patterns of 1032 pluripotent and somatic cell samples (left panel) and Nanog downregulation time course samples (right panel). The large ranges in the Pluripotency Scores and Lineage Scores in the left hand panel reflect the wide variety of cell types used to construct the classifier. The Nanog depletion time series represent the earliest stages of ES cell differentiation, and therefore, naturally show high Pluripotency Scores and low Lineage Scores. Nevertheless, a movement away from the pluripotent state is clearly detected using these classifiers; thus, highlighting their sensitivity and range. **(d)** Similarity matrix of samples in classification space. **(e)** PCA of the Nanog depletion time-course data (first two components are shown).

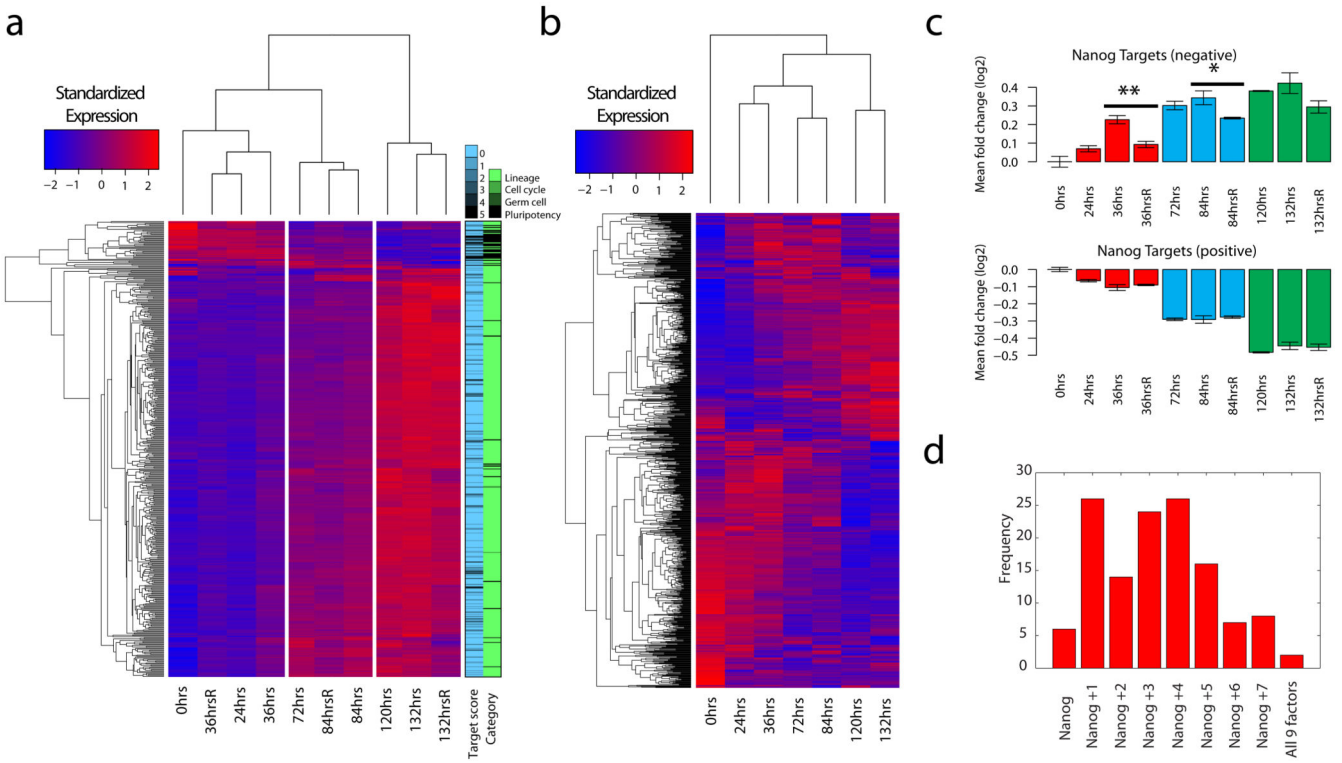

Figure 3. Expression changes and promoter occupancy by Nanog

(a) Hierarchical clustering of expression changes of pluripotency, lineage and cell cycle associated genes (see Supplementary Table S1). The blue bar shows the number of times each gene has been reported as a target of Nanog in six recent papers that examined promoter occupancy[20,48–52]. The green bar shows the category to which the genes belong. Pluripotency associated genes are frequently high confidence targets of Nanog. **(b)** Expression patterns for high confidence direct targets of Nanog. Genes were selected as high confidence Nanog targets if they were identified in at least three of six recent papers that examined Nanog target gene promoter occupancy[20,48–52]. **(c)** Mean fold changes for high confidence direct targets of Nanog. Expression patterns are not uniform, so mean fold changes are shown separately for those genes that were upregulated and downregulated during the time-course. Error bars show ± one standard error, $n = 3$. **(d)** The total number of Nanog target genes that changed significantly after Nanog depletion along with the number of other ES cell TRN members that also regulate that gene. Most commonly, Nanog regulates expression in concert with 1 to 5 other transcription factors.

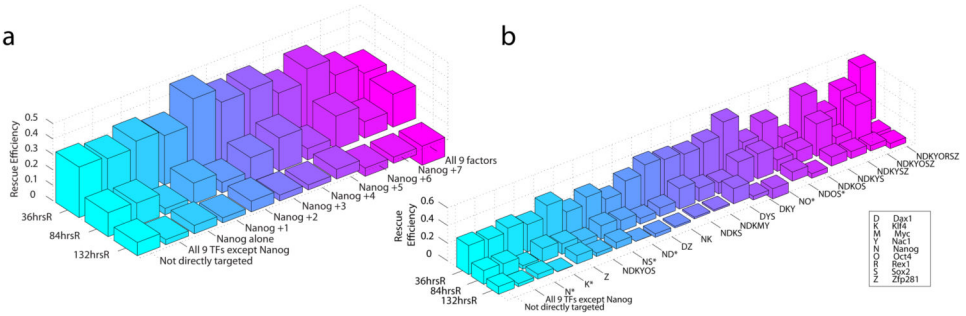

Figure 4. Gene expression changes are regulated in a highly combinatorial manner

Rescue efficiency (see online Methods) plotted against rescue time. Genes are grouped by: **(a)** the total number of factors in the ES TRN which directly regulate their expression and **(b)** the most significant regulatory combinations (odds-ratio > 1, Fisher exact test *p*-value < 0.05, and 3 or more target genes). Stars highlight combinations that correspond to feedback loops in the ES cell TRN. A few combinations (Nanog + 6, Nanog + 7, All 9 factors, in panel **a**; DZ, DKY, NO, NDKOS, NDKORSZ, in panel **b**) have negative rescue efficiency at the later time-points, indicating that Nanog reintroduction resulted in further movement away (rather than back toward) to the initial state. Promoter occupancy data is from Ref. 20

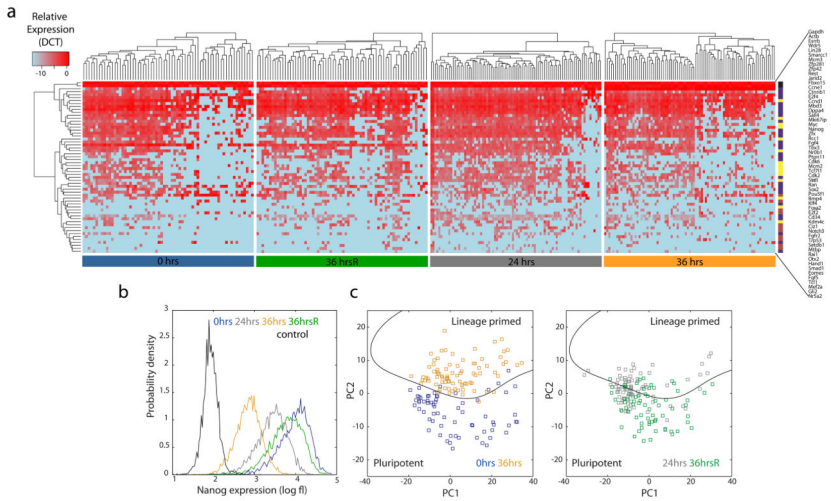

Figure 5. Single cell gene expression patterns

(a) Heat maps of single cell expression profiles. Highly expressed genes are in red; absent (not expressed) genes are in light blue. The coloured sidebar identifies the following classes of genes: housekeeping genes (black); pluripotency associated genes (purple); cell cycle associated genes (yellow); lineage associated genes (brown). **(b)** Flow-cytometric analysis of Nanog expression levels during transient Nanog downregulation. **(c)** SVM classification of single cell expression profiles plotted in the first two principal components. Training datasets (0hrs and 36hrs) are in the left panel and the 24hrs and 36hrsR datasets are in the right panel. In both panels, the black line separates the pluripotent and lineage primed classes.

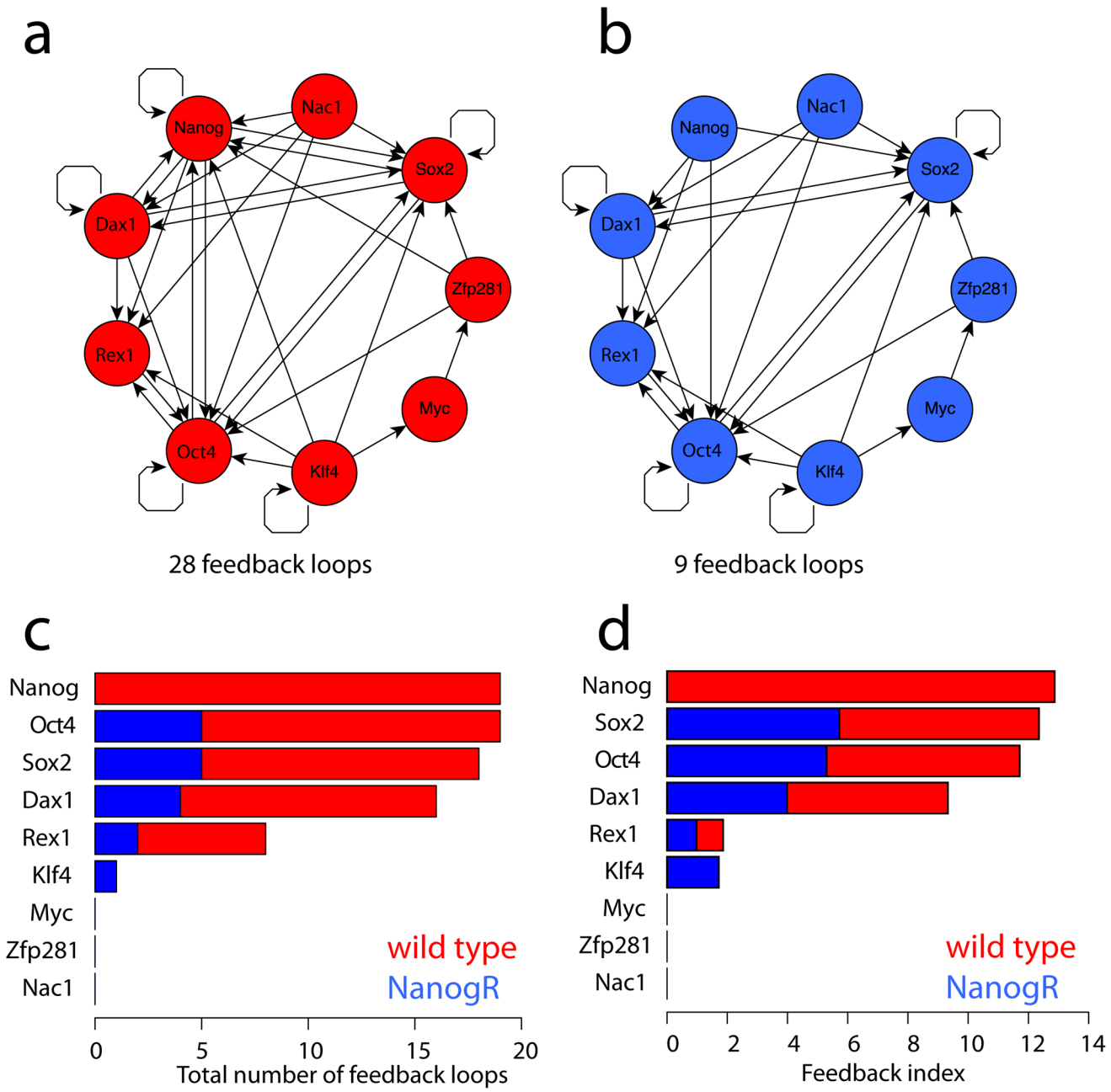

Figure 6. Feedback in the ES cell TRN

(a) The feedback-rich wild-type TRN. **(b)** The feedback-depleted NanogR TRN (+dox, Nanog active). **(c)** The total number of feedback loops that each transcription factor participates in is shown for the wild-type ES cell TRN (red) and NanogR TRN (blue). **(d)** Feedback centrality (as detailed in Refs. [45],[46]) for the wild-type ES cell TRN (red) and NanogR TRN (blue).

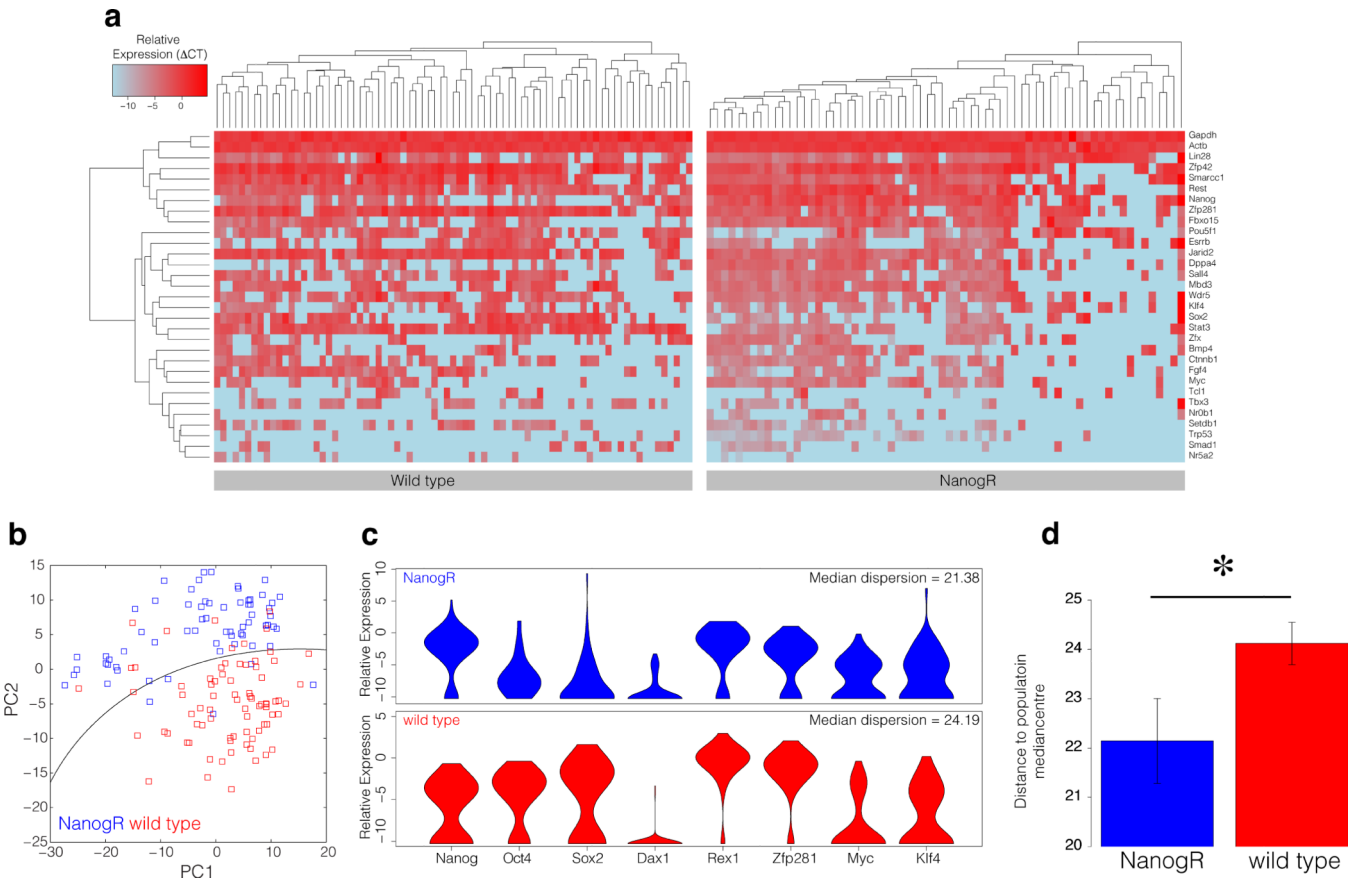

Figure 7. Cell-cell variability in wild-type and NanogR populations

(a) Heat maps of single cell expression profiles in wild-type CCE and NanogR ES cell populations. Highly expressed genes are in red; absent (not expressed) genes are in light blue. **(b)** SVM classification of NanogR and wild-type CCE mouse ES cells plotted in the first two principal components. The black line separates the NanogR and wild-type classes. **(c)** Violin plots of single cell relative expression levels in NanogR (blue) and wild-type CCE ES cells (red) for each factor in the extended ES cell TRN. Note, that these plots show expression variation but not covariance. In order to quantify overall (multivariate) variability, the median dispersion of the populations was calculated (see online Methods). Expression of Nac1 is not shown since it was not detected in sufficient numbers of cells in either NanogR or CCE ES cell populations to estimate its distribution. **(d)** The distance to mediancentre may be used as a test statistic to assess significant differences in overall (multivariate) variability in NanogR and wild-type CCE cells. The star indicates that the NanogR cells are significantly less variable as a population than the wild-type CCE ES cells ($p \leq 0.05$ by multivariate analogue of Levene's test). Error bars show ± one standard error, $n = 66$ (NanogR) and $n = 77$ (wild-type).